BIBECHANA
Vol. 22, No. 3, December 2025, 248-257

ISSN 2091-0762 (Print), 2382-5340 (Online)
Journal homepage: http://nepjol.info/index.php/BIBECHANA
Publisher:Dept. of Phys., Mahendra Morang A. M. Campus (Tribhuvan University)Biratnagar

Eco-friendly synthesis of silver nanoparticles using Withania somnifera root extract: characterization, phytochemical profiling, and evaluation of antimicrobial activity

Ratna Bahadur Thapa[1], Shankar Datt Ojha[2], Sujan Dhungana[2], Laxmi Tiwari[2], Devendra Khadka[3,4], Milan Babu Poudel[5], Megh Raj Pokhrel[4], Janaki Baral[2], Bhoj Raj Poudel[2*]

[1]*Department of Chemistry, Damak Multiple Campus,T.U., Damak Nepal*
[2]*Department of Chemistry, Tri Chandra Multiple Campus, T.U., Kathmandu, Nepal*
[3]*Department of Chemistry, Tribhuvan Multiple Campus, T.U., Tansen, Palpa, Nepal*
[4]*Central Department of Chemistry, T.U,Kirtipur, Kathmandu, Nepal*
[5]*Department of Convergence Technology Engineering, Jeonbuk National University, Jeonju, jeollabuk-do 54896,Republic of Korea*
[*]Corresponding author. Email: bhoj.poudel@trc.tu.edu.np

Abstract

Silver nanoparticles (Ag NPs) were synthesized using a green chemistry approach, utilizing Withania somnifera *(Ashwagandha) root extract, whose phytochemicals acted as eco-friendly, non-toxic reducing agents. The synthesized AgNPs were characterized using X-ray diffraction (XRD), UV-visible spectroscopy, Fourier transform infrared spectroscopy (FTIR), scanning electron microscopy (SEM) and energy dispersive X-ray spectroscopy (EDS). XRD analysis confirmed the crystal structure of the Ag NPs and estimated their size to be 10 nm. UV-visible spectroscopy showed a characteristic absorption peak, confirming the formation of AgNPs. FTIR analysis identified functional groups associated with the phytochemicals in the root extract, which may contribute to nanoparticle stabilization. SEM images revealed the spherical morphology of the Ag NPs, while EDS analysis confirmed the presence of silver in the synthesized nanoparticles. The phytochemical examination of Ashwagandha found secondary metabolites, including phenolic, alkaloid, and flavonoid compounds. The synthesized Ag NPs were assessed for their antimicrobial activity against* Staphylococcus aureus, Escherichia coli, *and* Candida albicans, *demonstrating significant efficacy markedly against Gram-positive bacteria. This finding highlights the role of Ashwagandha-mediated Ag NPs in sustainable NP formation and antimicrobial applications.*

Keywords
Antimicrobial activity, phytochemical analysis, root extract, Ag NPs, *Withania somnifera.*

Article information
Manuscript received: March 9, 2025; Revised: August 5, 2025; Accepted: August 8, 2025
DOI https://doi.org/10.3126/bibechana.v22i3.76471

1 Introduction

Nanoscience involves the investigation and modification of materials on a nanoscale, generally defined as being between 1 and 100 nanometers (nm). Nanoscience has rapidly evolved and gained considerable attention in research with industry worldwide [1]. Nanoparticles (NPs) exhibit distinct electrical, optical, chemical, and catalytic characteristics that set them apart from larger bulk substances, making them highly important for many applications [2,3]. Bio-nanotechnology is the backbone of nanotechnology; it combines biotechnology and nanotechnology to develop eco-friendly and biosynthetic methods for synthesizing nanomaterials [4]. Metallic NPs, including AgNPs, gold, titanium, copper, and zinc, are widely studied for their superior performance in various applications. AgNPs are widely recognized for their potent antimicrobial activity, which makes them highly valuable across many fields, including medicine, food science, agriculture, and environmental remediation. Their effectiveness stems from their ability to inhibit microbial growth, contributing to advancements in numerous applications [5,6].

The process of synthesizing AgNPs has advanced over time, with earlier chemical reduction techniques frequently using harmful chemicals that present health and environmental hazards [7]. In response, green or eco-friendly synthesis methods have gained attention, utilizing natural materials such as plant extracts, microbes, and biopolymers to create NPs without harmful chemicals, making the process more secure and environmentally friendly [8]. AgNPs exhibit multifunctional properties that have led to their widespread applications in medicine, catalysis, and environmental remediation [9,10]. Compared to metals like gold and platinum, silver offers cost-effective and scalable synthesis, particularly when biosynthetic routes are adopted. Furthermore, biosynthetic methods using plant-derived compounds such as polyphenols and proteins as reducing agents enhance the environmental friendliness and cost-efficiency of Ag NPs formation [11]. However, challenges related to scalability, cost, and labour intensity remain in NP synthesis.

Withania somnifera is widely recognized as Ashwagandha (**Figure 1**). It contributes to Ayurvedic medicine and is renowned for its numerous positive health effects, including anti-swelling, oxidative stress-reducing, adaptogenic, and antimicrobial [12]. With its ability to thrive in arid regions and poor soils, Ashwagandha is widely cultivated in India, Nepal, the Middle East, and parts of Africa [13]. The utilization of plentiful natural resources, including botanical extracts, further emphasizes the potential of green synthesis techniques. The plant is rich in various bioactive entities that enhance its therapeutic benefits [14]. Among many plant-based sources, Ashwagandha has emerged as an intriguing candidate for the synthesis of AgNPs.

Figure 1: Arial part and root of *Withania somnifera* (Ashwagandha) plant.

The eco-friendly Ag NPs synthesis using *Withania somnifera* root extract presents a sustainable alternative to conventional methods, harnessing the plant's natural phytochemicals for both reduction and stabilization. This method supports environmental sustainability and can elevate the antimicrobial properties of AgNPs by leveraging the synergistic interaction with bioactive compounds derived from plants [15]. This finding explores the synthesis of AgNPs using *Withania somnifera* root extract. Research highlighted the characterization, phytochemical profile, and antimicrobial properties of the NPs. Various analytical techniques, including XRD, SEM, and UV-visible spectroscopy, will be utilized to assess the size, morphology, and Ag NPs' stability. The phytochemical composition of *Withania somnifera* compounds will be examined to lead to the formation of NPs. Additionally, Ashwagandha-based AgNPs of antimicrobial activity will be assessed against bacterial, fungal, and viral pathogens, aiming to evaluate their potential applications in medical and biotechnological fields. The findings of this research will further promote the use of plant-based materials in NP synthesis, offering novel solutions for creating safe, efficient, and sustainable nanomaterials.

2 Materials and Methods

2.1 Materials

In the laboratory experiments, distilled water and analytical-grade chemicals were utilized. Silver nitrate ($AgNO_3$), and sodium hydroxide (NaOH) were obtained from Thermo Fisher Scientific India Pvt. Ltd., India.

2.2 Collection and preparation of Ashwagandha root extract

The roots of Ashwagandha plant were collected from their natural habitat in Tapoban forest of

Marma Rural Municipality-4, Darchula district, Sudurpashchim Province, Nepal (29.738° N, 80.821° E) between March and April 2024. The plant was harvested during the cooler morning hours. The roots were carefully washed with clean water, then sliced into smaller segments and allowed to dry in a shaded area for two weeks. After the drying period, the roots were processed into a fine powder using a mechanical grinder. For the extraction, 10 grams of the powdered Ashwagandha were soaked with 100 mL distilled water in a beaker. The solution was heated to 60° C and stirred for 30 minutes with a magnetic stirrer. Afterwards, the mixture was allowed to cool to a suitable temperature, filtered using Whatman filter paper, and stored at 4°C for later use.

2.3 Phytochemical screening

The hydro-methanolic root extract, prepared by the cold percolation of 30 g of powder, yielded 12 g of crude methanolic extract, which was subsequently used for the qualitative screening of phytochemicals. The analysis followed established protocols incorporating slight modifications based on insights from earlier studies [16–18].

2.4 Synthesis of AgNPs

AgNPs were synthesized using a green method under optimized conditions. A 0.001 M AgNO solution was prepared by dissolving 0.17 grams of AgNO in 1000 mL of distilled water. In a typical reaction, 50 mL of this solution was mixed with 20 mL of freshly prepared Ashwagandha root extract, added dropwise under continuous magnetic stirring at 600 rpm. The reaction was conducted at ambient temperature (˜25 °C) and a neutral pH of 7.0, maintained by not adding any acid or base. The total reaction time was 30 minutes, during which the color change from pale yellow to dark brown indicated the formation of AgNPs. These parameters were selected based on reported optimal conditions for plant-extract-mediated silver nanoparticle synthesis.

2.5 Characterization of AgNPs

2.5.1 UV-vis spectroscopy

When materials absorb ultraviolet and visible light (200–600 nm), they produce the ultraviolet-visible spectrum. The AgNPs produced using Ashwagandha root extract were characterized by a UV-visible spectrophotometer (Specord 200 Plus, Analytik, Jena, Germany).

2.5.2 XRD analysis

The crystallographic information of synthesized AgNPs was investigated using a D2 phaser, Bruker with Cu K radiation. The scanning was performed over a 2 range of 30°-90° utilizing a step size of 0.2003

2.5.3 FTIR analysis

FTIR analysis was conducted using a PerkinElmer spectrometer with Spectrum IR (Version 10.6.2 to determine the functional groups found in the root extract responsible for the synthesis of Ag NPs within the spectral range of 500-4000 cm^1.

2.5.4 FE-SEM and EDS analysis

The morphology and elemental composition of AgNPs were analyzed using a field emission scanning electron microscope (FE-SEM, Hitachi, Japan) equipped with an energy-dispersive X-ray spectroscopy (EDS) detector.

2.6 Antimicrobial effectiveness

The antimicrobial effectiveness of AgNPs and root extract was evaluated against three specific microbial strains: *Escherichia coli* (ATCC 8739), which is a Gram-negative bacterium; *Staphylococcus aureus* (ATCC 6538P), a Gram-positive bacterium; and *Candida albicans* (ATCC 2091), a fungal organism. The assessment utilized the agar-well diffusion technique to compare their effectiveness with that of a standard antibiotic. Each culture was incubated under optimal conditions, ensuring precise measurement of inhibition zones and clear differentiation between microbial responses. All antimicrobial experiments were conducted in triplicates. The data are expressed as mean ± standard deviation (n=3).

2.6.1 Media preparation

A liquid broth (LB) medium was made by mixing 13 grams of LB powder (from Sisco Research Laboratories Pvt. Ltd., India) into 1 litre of distilled water. This mixture was subsequently sterilized in an autoclave set at 121°C and 15 psi for 25 minutes. After sterilization, it was allowed to cool to 50 °C. Once cooled, 5 mL portions of the medium were aseptically distributed into pre-sterilized 15 mL Falcon tubes. The tube was then inoculated with a bacterial culture and incubated for 1 day for bacterial cell growth. To ensure accuracy and reproducibility, it is crucial to maintain aseptic techniques throughout the process and to verify that the incubation conditions are optimal for the specific bacterial strains being studied.

2.6.2 Media Plated and Antimicrobial Assay Preparation

Muller Hinton Agar (MHA) plates were made by dissolving 39 grams of MHA powder (Sisco Research Laboratories Pvt. Ltd., India) in one litre of distilled water. After mixing, the solution was sterilized in an autoclave at 121°C and a pressure of 15 psi for 25 minutes. Following autoclaving, the medium was allowed to cool to approximately 50°C before being dispensed into sterile Petri dishes, with each plate receiving 25 mL of the prepared agar. Before the antimicrobial assay, each plate (stored in the refrigerator) was labelled with the corresponding sample name. By using a sterile cotton swab, a 150 µL aliquot of bacterial suspension was spread evenly on the surface of the agar. Wells were then created in the agar to accommodate the test samples and standards. For plant extracts, samples were loaded with 50 mg/mL concentration dissolved in DMSO, while NPs were added at approximately 30 mg per well. A kanamycin solution (5 mg/mL; 10 µL) was used as a positive control to assess bacterial strain comparability. Similarly, for antifungal evaluation, itraconazole (20 mg/mL; 10 µL) was introduced into the designated wells as a standard reference. The plates were incubated at 37°C for 24 hours, and the effects were evaluated.

2.7 Data analysis

The data obtained was analyzed and plotted using Origin 2024b software.

3 Results and Discussion

3.1 Phytochemical screening

The phytochemical components in the Ashwagandha root extract that contributed to the reduction and stabilization of AgNPs were analyzed qualitatively. Results of phytochemical screening indicate that hydro-methanolic root extract is rich in secondary metabolites (test result in **Table 1)**. Alkaline reagent tests were done in the presence of flavonoids [17], and alkaloids were found using Hager's test [18]. The test showed positive results for saponins, as indicated by the Froth test [17]. Terpenoids and steroids were also detected through positive results in the Salkowski test [18]. Tannins were presented as evidenced by the lead acetate test [18]. Additionally, quinone was identified through the concentrated hydrochloride (HCl). The presence of glycosides and phenolic compounds was confirmed using sodium hydroxide and ferric chloride tests [16]. These compounds, extracted with polar solvents, have an inherent polarity that aids in NP formation and stabilization.

Table 1: Phytochemical screening of the hydro-methanolic root extracts of *Ashwagandha*

S. N	Secondary metabolites	Tests	Result
1	Flavonoid test	Alkaline reagent test	+
2	Alkaloids test	Hager's test	+
3	Saponins test	Froth test	+
4	Terpenoids and Steroids test	Salkowski test	+
5	Tannins	Lead acetate test	+
6	Quinone test	Conc. HCl	+
7	Glycosides	NaOH	+
8	Phenolic	$FeCl_3$	+

Note: "+" indicates the presence of the phytochemical content.

3.2 Green synthesis of AgNPs

The environmentally friendly formation of AgNPs can be achieved using extracts from plants that are abundant in various bioactive substances, including phenolic acids, terpenoids, and proteins. These compounds serve as natural reducing agents in the synthesis process. These biomolecules aid in converting metal ions into stable NPs, offering a greener alternative that minimizes the use of harmful chemicals. These compounds help reduce metal salts to nanoscale particles, such as converting Ag^+ to Ag° in Ag NPs synthesis. Ashwagandha, known for its antioxidant properties, is particularly effective in reducing silver ions to AgNPs. In this process, an aqueous Ashwagandha extract is combined with AgNO under constant stirring. The bioactive compounds present in plant extract assist in the reduction of silver ions (Ag^+) by providing electrons, which results in the formation of AgNPs. This process often involves a noticeable colour change due to SPR, typically shifting the solution's colour to a shade of brownish-blue [19]. The neutral pH (~7) and ambient temperature maintained during the

synthesis likely favored the reduction kinetics and stabilization of AgNPs by phenolic and flavonoid constituents in the extract. The 30-minute reaction time aligns with other rapid green synthesis protocols reported in the literature [20]. **Figure 2** illustrates the green synthesis route of AgNPs using *Withania somnifera* root extract, showing the key steps: preparation of plant extract, reduction of Ag ions, and stabilization of nanoparticles by bioactive phytochemicals.

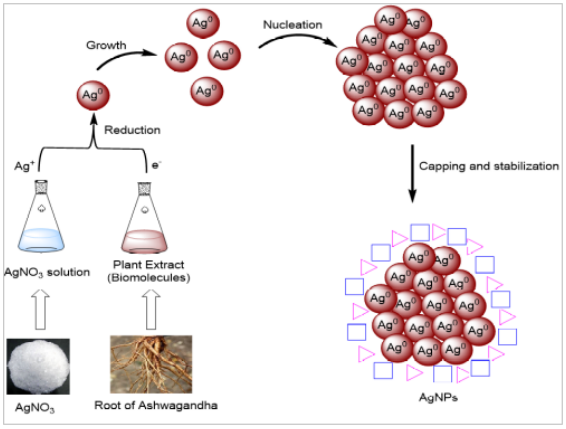

Figure 2: Representative diagram of green synthesis of Ag NPs.

3.3 Characterization of AgNPs

3.3.1 UV-vis spectroscopy analysis

Ag NPs synthesized using *Withania somnifera* root extract were confirmed through UV-vis spectroscopy, which displayed a broad absorption spectrum between 300–600 nm. A clear peak at 433 nm is observed, as illustrated in **Figure 3(a)**. The optical absorption peak observed at 433 nm corresponds to surface plasmon resonance (SPR), a hallmark feature of metallic AgNPs. The SPR peak arises from collective oscillation of conduction electrons on the nanoparticle surface in resonance with incident light [20]. The peak position varies based on the morphology and size of the NPs, with smaller particles generally exhibiting a blue shift. The broad spectral profile indicates a certain level of polydispersity, a common trait in green synthesis methods [21].

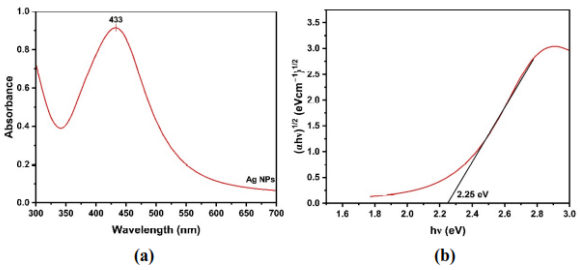

Figure 3: (**a**)Ultraviolet-visible absorption spectra (**b**) Tauc plot indicating an apparent optical energy gap (˜2.25 eV), derived from quantum confinement effects in AgNPs.

The energy gap of Ag NPs differs from that of macroscopic silver due to quantum confinement effects [22]. In bulk form, silver behaves as a metal with no band gap since the conduction and valence bands overlap. However, when silver is reduced to the nanoscale, especially at smaller particle sizes, a shift in optical properties resembling a band gap can develop. For Ag NPs, this energy gap typically ranges between 2.0 eV and 4.0 eV, affected by the surrounding and size conditions of the particle. This optical gap, observed through techniques like UV-visible spectroscopy, is linked to plasmonic resonances rather than the electronic bandgap found in semiconductors. However, band gap governs the material's electrical properties and is essential in determining whether a material behaves as a conductor, semiconductor, or insulator [23]. AgNPs energy gap (Eg) determined through the Tauc method [24, 25];

$$(\alpha h\nu)^{1/m} = C(h - Eg)$$

Here, = absorbance coefficient, C = constant, h = Planck's constant, = photon frequency, Eg = optical band gap, and m = $\frac{1}{2}$ for direct band gap semiconductors.

Additionally, an optical energy gap of 2.25 eV was calculated using the Tauc method (Figure 3 (b)). While this value mimics a "bandgap," it is not a true electronic bandgap as seen in semiconductors. Instead, it reflects quantum confinement effects and plasmonic behavior associated with the small size of AgNPs. As AgNPs are metallic, their conduction and valence bands overlap in bulk; however, at the nanoscale, localized surface effects and interaction with light can produce apparent optical transitions that resemble a bandgap [21, 22].

3.3.2 FTIR analysis

The analysis using FTIR was conducted to determine the functional groups that play a role in the synthesis and stabilization of Ag NPs. In **Figure 4**, the FTIR spectra of the plant extract is shown in

black, while those of the synthesized AgNPs are represented in red. In the FTIR spectrum of the plant extract, several distinctive peaks are observed, with a prominent absorption band at 3307 cm^1. The presence of hydroxyl groups in the extract has been indicated by the vibrations associated with O–H stretching [26]. The peak observed at 2940 cm^1 corresponds to asymmetric C–H stretching, suggesting that alkyl groups are present. Furthermore, the bands identified at 1607cm^1 and 1408 cm^1 are associated with C=C and C–H vibrations, respectively. Additionally, the spectrum feature at 1028 cm^1 is attributed to C–O stretching, a characteristic often associated with alcohols or phenolic compounds [27]. A band at 608 cm^1 was associated with C–H bending vibrations.

The presence of Ag NPs resulted in significant changes, with all spectral bands showing weaker intensity in comparison to the original plant extract. This indicates that Ag NPs were successfully formed. Notably, the reduced intensity of the O–H stretching vibration at 3307 cm^{-1} suggests that hydroxyl groups played a role in the synthesis of the NPs. Moreover, the shifts observed in the C=C (1593 cm^{-1}) and C–O (1016 cm^{-1}) absorption peaks provide further evidence of the involvement of these functional groups during the formation process. It is believed that various functional groups such as hydroxyl, and carbonyl are integral to not only the reduction of silver ions but also the stabilization of the NPs [28].

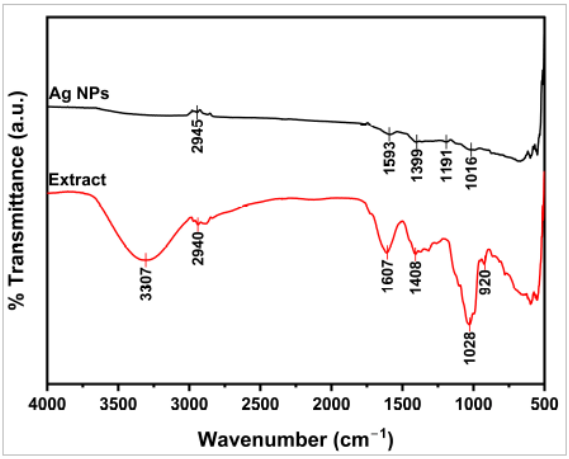

Figure 4: (FTIR spectra of AgNPs (black) and root extract (red).

3.3.3 XRD analysis

XRD is a powerful method used to examine the size and crystalline structure of materials by analyzing the diffraction patterns produced when X-rays interact with a sample. The crystalline structure of *Withania somnifera*-based Ag NPs was analyzed using XRD as shown in **Figure 5**. The observed diffraction peaks at 2 angles of 37.8°, 44.3°, 64.4°, 77.2° and 81.2° correspond to the Miller indices (111), (200), (220), (311) and (222) respectively. These peaks suggest the presence of a face-centred cubic (FCC) crystal structure. These results were validated by comparing them to the JCPDS database (file number: 01-087-0717) [29]. Some of the observed peaks were attributed to partial oxidation of silver, which occurred during long-term storage before characterization. The average crystallite size of powdered AgNPs was estimated using Scherrer's equation [30],

$$D = \frac{k\lambda}{\beta cos\ \theta}$$

In this eqn, the following variables are defined: D refers to the size of the crystallite or grain, K is the dimensionless shape factor, which is set at 0.9, represents the wavelength of the X-ray radiation being utilized, denotes Bragg's angle expressed in radians, and indicates the full width at half maximum, also measured in radians. The most intense diffraction peak appeared at 37.8°. The size of the crystallites in the AgNPs was measured to be 10.57 nm. This calculation was based on the XRD data, which includes detailed information on peak positions and angles, crucial for determining the crystallite size.

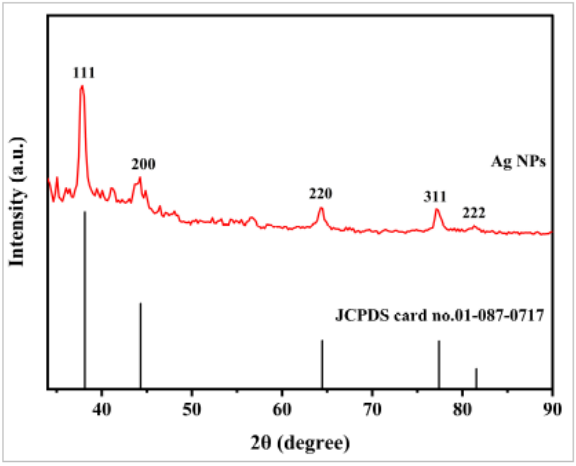

Figure 5: XRD patterns of Ag NPs.

3.3.4 SEM/EDS analysis

The surface features and elemental percentage of the formed Ag NPs were examined through SEM and energy-dispersive X-ray spectroscopy (EDS). SEM image captured at a scale bar of 0.5 m is presented in **Figure 6**, showing spherical particles with consistent size distribution and noticeable agglomeration of the Ag NPs. When Ag NPs are heated indirectly, they tend to cluster together, leading to the electronic coupling between the metal

particles. This interaction causes a shift in the SPR to higher wavelengths, accompanied by a higher intensity in the UV-visible spectrum, in contrast to the behaviour of individual particles [31]. The synthesis method, purification steps, and drying conditions are key factors affecting the agglomeration, dispersion, stability, and size distribution of Ag NPs [32].

Silver was found to be the most abundant element, comprising 56.9%, followed by carbon at 29.7%, and oxygen at 13.5%. A prominent peak confirmed the presence of silver metal. The peaks corresponding to oxygen and carbon, as seen in **Figure 6**, are attributed to organic components from the proteins or enzymes in the extract, as well as the carbon tape used during the measurement process [33].

3.4 Antimicrobial Evaluation

The agar diffusion method was used to perform antimicrobial activity, adhering to established guidelines [34]. The Zone of Inhibition (ZOI) served as the primary indicator to gauge antimicrobial effectiveness. The size of the ZOI created on bacterial cultures was assessed to determine the antimicrobial activity of plant extracts, as shown in **Table 2**. The ZOI for each microbial strain was measured in millimeters and reported as mean ± SD (n = 3). ATCC (American Type Culture Collection) was the source for the microbial reference strains that play an essential role in standardizing and distributing these materials, ensuring reproducibility and reliability across scientific research and industrial applications.

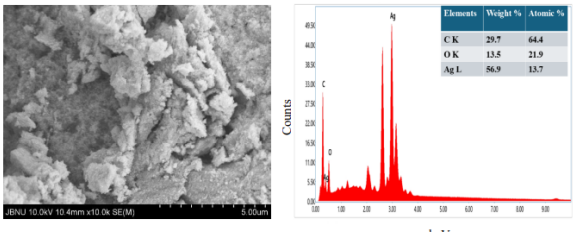

Figure 6: SEM image and EDS spectrum of synthesized Ag NPs.

Table 2: Antimicrobial screening of *Withania somnifera* extracts

Strain	Reference culture	Type	Control (c^+) (mm)	Ag NPs (mm)	Plant extract (mm)
E. coli	ATCC8739	Gram-negative	25.0 ± 0.4	21.3 ± 0.4	0.0
S. aureus	ATCC6538P	Gram-positive	26.1 ± 0.4	22.4 ± 0.4	0.0
C. albicans	ATCC2091	Fungi	27.2 ± 0.4	20.2 ± 0.4	0.0

Note: ZOI = Zone of inhibition in mm. Kanamycin (positive control, c^+), concentration of 5 mg/mL. DMSO was used as a negative control and showed no activity.

The antimicrobial activity of Ashwagandha extract on *E. coli* was tested using the ATCC 8739 reference strain, with a positive control for comparison. The positive control produced a ZOI of 25 mm, while Ag NPs exhibited a ZOI of 21 mm against the strain, shown in **Figure 7(a)**, which suggests that Ag NPs demonstrate considerable antibacterial properties against *E. coli*. The antimicrobial effect of Ashwagandha extract against *S. aureus* was assessed using the ATCC 6538P reference strain, with a positive control for comparison. The ZOI for positive control was 26 mm, while AgNPs showed a ZOI of 22 mm against this strain, as shown in **Figure 7(b)**. These findings demonstrate that Ag NPs have significant antibacterial activity against *S. aureus*. Antimicrobial activity of AgNPs possesses notable antimicrobial activity against *C. albicans* which was tested using the ATCC 2091 reference strain, with a positive control for comparison. The ZOI for the positive control was 27 mm, while AgNPs showed a ZOI of 20 mm against this strain, as depicted in **Figure 7(c)**.

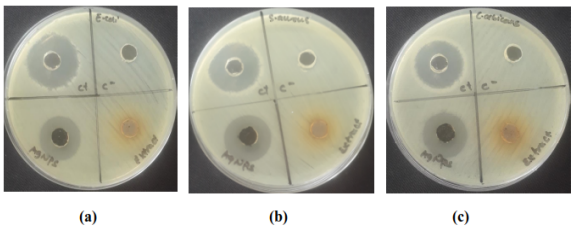

(a) (b) (c)

Figure 7: Zone of Inhibition for (**a**) *E. coli,* (**b**) *S. aureus, and* (**c**) *C. albicans.*

3.5 Antibacterial Mechanism of AgNPs

AgNPs exhibit antimicrobial properties through both direct and indirect mechanisms. A key factor in their effectiveness is the continuous release of Ag, which plays a crucial role in bacterial inhibition. These ions have a strong affinity towards proteins, allowing them to attach to bacterial cell walls and membranes, **Figure 8**. This interaction disrupts membrane integrity, increasing permeability and leading to structural instability. Once silver ions enter the cell, they disrupt the activity of respiratory enzymes, leading to the production of

reactive oxygen species (ROS) and hindering the synthesis of ATP. The oxidative stress caused by ROS damages essential cellular components, including lipids, proteins, and DNA [35]. Additionally, silver ions bind to DNA, disrupting replication and transcription, which hampers cell division and ultimately leads to bacterial death [36]. They also interfere with ribosomal function, inhibiting protein synthesis and disrupting cellular processes [37, 38].

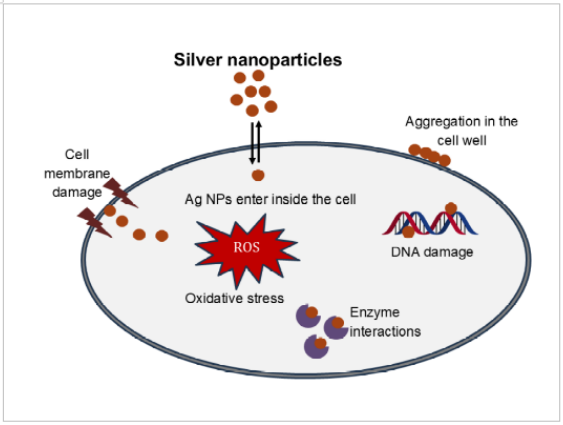

Figure 8: Mechanism for the antimicrobial activity of Ag NPs..

Beyond ion release, Ag NPs themselves contribute to bacterial inhibition. When bacteria encounter certain substances, they gather on their surfaces and infiltrate the cell wall. This infiltration disrupts the internal structures and causes the leakage of cellular materials, ultimately leading to cell death. Moreover, Ag NPs interfere with bacterial signaling pathways by dephosphorylating tyrosine residues on peptide substrates, disrupting essential regulatory functions. This disruption inhibits bacterial proliferation and promotes cell death. Through this combination of silver ion activity, nanoparticle interaction, and interference with cellular functions, Ag NPs demonstrate broad-spectrum antimicrobial efficacy [39, 40].

4 Conclusions

Ag NPs synthesis using Ashwagandha root extract provides an environmentally friendly and effective method for NP formation. The synthesized nanoparticles were characterized through UV-Vis spectroscopy, FTIR, XRD, and SEM/EDS; this led to the formation of NPs that were spherical and crystalline in shape, measuring 10.57 nm in size. Ag NPs are stabilized by phytochemicals, including alkaloids, saponins, and phenolic compounds found in the extract. The NPs exhibited enhanced antimicrobial effectiveness against Gram-positive and Gram-negative bacteria, displaying larger inhibition zones and reduced MIC values compared to the extract on its own. These results underscore the potential of Ashwagandha-derived Ag NPs for medical and environmental purposes, highlighting the significance of green synthesis in promoting sustainable nanotechnology. Future studies should aim to refine synthesis conditions and investigate additional applications to fully exploit the capabilities of these NPs. Future research will focus on finding the Quantitative phytochemical profiling. This study had some limitations, lack of quantitative phytochemical data and potential variability in extract composition. To gain a better understanding of the mechanistic role of bioactives in the synthesis of Ag NPs, future studies should incorporate quantitative estimation of the total phenolic/flavonoid content and HPLC/GC-MS profiling.

Acknowledgments

The first author (R.B. Thapa) acknowledges funding support from Mini Research Grant (Grant No. 2/2081), Tribhuvan University, Institute of Science and Technology (IoST), Dean's office, Kathmandu, Nepal

Conflicts of Interest

The authors declare that there are no conflicts of interest associated with the publication of this research paper.

References

[1] I. Khan, K. Saeed, and I. Khan. Nanoparticles: Properties, applications and toxicities. *Arab. J. Chem.*, 12(7):908–931, 2019.

[2] X. Cui et al. Photothermal nanomaterials: A powerful light-to-heat converter. *Chem. Rev.*, 123(11):6891–6952, 2023.

[3] Y. Fu et al. Applications of nanomaterial technology in biosensing. *J. Sci-Adv. Mater. Dev.*, 9(2):100694, 2024.

[4] A. Karnwal et al. Gold nanoparticles in nanobiotechnology: From synthesis to biosensing applications. *ACS Omega*, 9(28):29966–29982, 2024.

[5] A. Dhaka, S. Chand Mali, S. Sharma, and R. Trivedi. A review on biological synthesis of silver nanoparticles and their potential applications. *Res. Chem.*, 6:101108, 2023.

[6] G. E. Yılmaz, I. Göktürk, M. Ovezova, F. Yılmaz, S. Kılıç, and A. Denizli. Antimicrobial nanomaterials: A review. *Hygiene*, 3(3):269–290, 2023.

[7] A. S. Rodrigues et al. Advances in silver nanoparticles: a comprehensive review on their potential as antimicrobial agents and their mechanisms of action elucidated by proteomics. *Front. Microbiol.*, 15:1440065, 2024.

[8] B. Bhardwaj, P. Singh, A. Kumar, S. Kumar, and V. Budhwar. Eco-friendly greener synthesis of nanoparticles. *Adv. Pharm. Bull.*, 10(4):566–576, 2020.

[9] H. A. Hussein and M. A. Abdullah. Novel drug delivery systems based on silver nanoparticles, hyaluronic acid, lipid nanoparticles and liposomes for cancer treatment. *Appl. Nanosci.*, 12(11):3071–3096, 2022.

[10] M. Rafique, I. Sadaf, M. S. Rafique, and M. B. Tahir. A review on green synthesis of silver nanoparticles and their applications. *Artif. Cells Nanomed. Biotechnol.*, 45(7):1272–1291, 2017.

[11] M. Fahim, A. Shahzaib, N. Nishat, A. Jahan, T. A. Bhat, and A. Inam. Green synthesis of silver nanoparticles: A comprehensive review of methods, influencing factors, and applications. *JCIS Open*, 16:100125, 2024.

[12] N. J. Dar, A. Hamid, and M. Ahmad. Pharmacologic overview of withania somnifera, the indian ginseng. *Cell. Mol. Life Sci.*, 72(23):4445–4460, 2015.

[13] P. Mikulska et al. Ashwagandha (withania somnifera)—current research on the health-promoting activities: A narrative review. *Pharmaceutics*, 15(4):1057, 2023.

[14] S. Shinde, A. K. Balasubramaniam, V. Mulay, G. Saste, A. Girme, and L. Hingorani. Recent advancements in extraction techniques of ashwagandha (withania somnifera) with insights on phytochemicals, structural significance, pharmacology, and current trends in food applications. *ACS Omega*, 8(44):40982–41003, 2023.

[15] T. Muthu et al. Eco-biofabrication of silver nanoparticles from azadirachta indica, gymnema sylvestre, and moringa oleifera for lung cancer treatment. *J. Egypt. Natl. Canc. Inst.*, 37(1):1, 2025.

[16] S. Dubale, D. Kebebe, A. Zeynudin, N. Abdissa, and S. Suleman. Phytochemical screening and antimicrobial activity evaluation of selected medicinal plants in ethiopia. *JEP*, 15:51–62, 2023.

[17] K. Godlewska, P. Pacyga, A. Najda, and I. Michalak. Investigation of chemical constituents and antioxidant activity of biologically active plant-derived natural products. *Molecules*, 28(14):5572, 2023.

[18] N. Kancherla, A. Dhakshinamoothi, K. Chitra, and R. B. Komaram. Preliminary analysis of phytoconstituents and evaluation of anthelminthic property of cayratia auriculata (in vitro). *Maedica*, 14:4, 2019.

[19] O. R. Bolduc and J.-F. Masson. Advances in surface plasmon resonance sensing with nanoparticles and thin films: Nanomaterials, surface chemistry, and hybrid plasmonic techniques. *Anal. Chem.*, 83(21):8057–8062, 2011.

[20] K. Ssekatawa et al. Green strategy–based synthesis of silver nanoparticles for antibacterial applications. *Front. Nanotechnol.*, 3:697303, 2021.

[21] M. J. Huber et al. Physicochemical characterization and quantification of nanoplastics: applicability, limitations and complementarity of batch and fractionation methods. *Anal. Bioanal. Chem.*, 415(15):3007–3031, 2023.

[22] N. Kh. Abdalameer, K. A. Khalaph, and E. M. Ali. Ag/ago nanoparticles: Green synthesis and investigation of their bacterial inhibition effects. *Materials Today: Proceedings*, 45:5788–5792, 2021.

[23] N. Chouhan. Silver nanoparticles: Synthesis, characterization and applications. In K. Maaz, editor, *Silver Nanoparticles - Fabrication, Characterization and Applications*. InTech, 2018.

[24] J. Baral et al. Green synthesis of copper oxide nanoparticles using mentha (mint) leaves characterization and its antimicrobial properties with phytochemicals screening. *J. Nepal Chem. Soc.*, 45(1):111–121, 2025.

[25] S. Dhungana et al. Synthesis and characterization of copper oxide nanoparticles isolated from acmella oleracea and study of antimicrobial and phytochemical properties. *Amrit Res. J.*, 5(1):18–29, 2024.

[26] S. Shrestha, L. Tiwari, S. Dhungana, J. Maharjan, D. Khadka, A. A. Kim, M. R. Pokhrel, J. Baral, M. Park, and B. R. Poudel. Exploring photocatalytic, antimicrobial and antioxidant efficacy of green-synthesized zinc oxide nanoparticles. *Nanomaterials*, 15(11):858, 2025.

[27] L. Rudi, I. Zinicovscaia, L. Cepoi, T. Chiriac, D. Grozdov, and A. Kravtsova. The impact of silver nanoparticles functionalized with spirulina protein extract on rats. *Pharmaceuticals*, 17(9):1247, 2024.

[28] P. Kuppusamy, S. Kim, S.-J. Kim, and K.-D. Song. Antimicrobial and cytotoxicity properties of biosynthesized gold and silver nanoparticles using d. brittonii aqueous extract. *Arab. J. Chem.*, 15(11):104217, 2022.

[29] R. S. Sancheti et al. Cordia sebestena leaf extract mediated biosynthesis of silver nanoparticles, characterization, and screening of its antimicrobial activities. *Green Anal. Chem.*, 6:100075, 2023.

[30] B. R. Poudel, L. Tiwari, C. Magar, S. Dhungana, A. R. Poudel, D. Khadka, M. R. Pokhrel, and J. Baral. Eco-friendly synthesis of zinc oxide nanoparticle using centella asiatica: phytochemical analysis, characterization and antimicrobial activity assessment. *Scientific World*, 18(18):39–46, 2025.

[31] P. Bhuyar, M. H. Ab. Rahim, S. Sundararaju, R. Ramaraj, G. P. Maniam, and N. Govindan. Synthesis of silver nanoparticles using marine macroalgae padina sp. and its antibacterial activity towards pathogenic bacteria. *Beni-Suef Univ. J. Basic Appl. Sci.*, 9(1):3, 2020.

[32] L. Xu, Y.-Y. Wang, J. Huang, C.-Y. Chen, Z.-X. Wang, and H. Xie. Silver nanoparticles: Synthesis, medical applications and biosafety. *Theranostics*, 10(20):8996–9031, 2020.

[33] L. N. Khanal et al. Green synthesis of silver nanoparticles from root extracts of rubus ellipticus sm. and comparison of antioxidant and antibacterial activity. *Journal of Nanomaterials*, 2022:1832587, 2022.

[34] T. J. Hossain. Methods for screening and evaluation of antimicrobial activity: A review of protocols, advantages, and limitations. *EuJMI*, 14(2):97–115, 2024.

[35] S. Anees Ahmad et al. Bactericidal activity of silver nanoparticles: A mechanistic review. *Mat. Sci. Ener. Tech.*, 3:756–769, 2020.

[36] S. Tang and J. Zheng. Antibacterial activity of silver nanoparticles: Structural effects. *Adv. Healthcare Materials*, 7(13):1701503, 2018.

[37] N. Durán, M. Durán, M. B. De Jesus, A. B. Seabra, W. J. Fávaro, and G. Nakazato. Silver nanoparticles: A new view on mechanistic aspects on antimicrobial activity. *NBM*, 12(3):789–799, 2016.

[38] B. R. Poudel, S. Dhungana, A. Dulal, A. R. Poudel, L. Tiwari, D. Khadka, M. R. Pokhrel, M. B. Poudel, A. A. Kim, and J. Baral. Eco-friendly fabrication of zinc oxide nanoparticles using gaultheria fragrantissima: Phytochemical analysis, characterization, and antimicrobial potential. *Inorganics*, 13(7):247, 2025.

[39] I. X. Yin, J. Zhang, I. S. Zhao, M. L. Mei, Q. Li, and C. H. Chu. The antibacterial mechanism of silver nanoparticles and its application in dentistry. *IJN*, 15:2555–2562, 2020.

[40] P. Kharel, M. D. Manandhar, S. K. Kalauni, S. Awale, and J. Baral. Isolation, identification and antimicrobial activity of a withanolide [ws-1] from the roots of withania somnifera. *Nepal J. Sci. Technol.*, 12:179–186, 2011.